Role of Oxygen Functional Groups in Carbon Nanotube/Graphene Freestanding Electrodes for High Performance Lithium Batteries

*Hye Ryung Byon, Betar M. Gallant, Seung Woo Lee, and Yang Shao-Horn**

Hierarchical functionalized multiwalled carbon nanotube (MWNT)/graphene structures with thicknesses up to tens of micrometers and relatively high density (>1 g cm^{-3}) are synthesized using vacuum filtration for the positive electrode of lithium batteries. These electrodes, which are self-standing and free of binder and current collectors, utilize oxygen functional groups for Faradaic reactions in addition to double-layer charging, which can impart high gravimetric (230 Wh kg^{-1} at 2.6 kW kg^{-1}) and volumetric (450 Wh L^{-1} at 5 kW L^{-1}) performance. It is demonstrated that the gravimetric and volumetric capacity, capacitance, and energy density can be tuned by selective removal of oxygen species from as-prepared functionalized MWNT/graphene structures with heat treatments in H_2/Ar, potentially opening new pathways for the design of electrodes with controlled surface chemistry.

1. Introduction

The increasing demand for energy storage devices for applications such as load-leveling of electrical energy supply and demand,[1] propulsion for electric vehicles, and microelectromechanical devices has motivated the search for new classes of electrode materials that provide high energy, high power, and long cycle life beyond what is possible from state-of-the-art lithium-ion batteries[2,3] or electrochemical capacitors (ECs).[4–6] Owing to advantages such as high electronic conductivity, good mechanical and chemical stability, unique material structures, and high specific surface areas, nanocarbons such as carbon nanotubes[2,4,7–9] and graphene[10–16] are receiving increasing attention as promising next-generation energy storage materials for ECs and lithium-ion batteries. However, despite a significant power advantage compared to lithium-ion batteries, in which the entire electrode active mass can be used to store charge via intercalation, the energy densities of nanocarbon-based electrodes remain relatively low owing to the limitations of double-layer charge storage, which confines charge and energy storage to only the surface of active materials. Further, incorporation of nanocarbons into electrodes remains challenging, and typically requires the addition of insulating binder, which imparts mechanical stability but can block the active surface of materials. Additionally, the high packing density desired from electrodes to enable high volumetric energy and power is difficult to achieve using traditional electrode synthesis processes. Therefore, new electrode designs for lithium storage materials must be coupled with suitable fabrication processes in order to develop promising and practical next-generation materials.

Recent efforts to develop improved carbon electrodes have employed various strategies, ranging from the continued development of more conventional high surface area activated carbons[5,17–19] including novel inkjet printing fabrication techniques,[18] to carbon onions for patterned microelectrodes,[20] to engineering of carbons with controlled pore sizes for increased gravimetric and volumetric capacitances utilizing carbide-derived carbons.[21–23] For carbon nanotube (CNT)-based electrodes, reports of novel structures of aligned carpets[7,24] or carbon nanotube papers[8] look promising for enabling good rate performance, although the density of aligned carpets (<0.6 g cm^{-3})[7,24] is low, yielding low volumetric capacitances (<100 F cm^{-3})[7,24]. In contrast, while graphene-based electrodes[10,11,14] offer the potential for higher densities owing to tight stacking of graphene sheets, close stacking can prevent ions from accessing the surface area and limit performance at high power. Therefore, a major challenge with graphene-based electrodes is developing novel structures that allow access to the surface area of graphene by incorporating sufficient porosity, for example by utilizing spacers such as carbon spheres[25,26] between graphene sheets to increase the spacing distance, which were shown recently to increase the capacitance of graphene electrodes by 70% in aqueous. Recent work by Ruoff et al.[27] reported microwave exfoliated graphite oxide that can attain high gravimetric capacitances of ≈170 F g^{-1} with high rate performance, albeit with low volumetric capacitance due to low density (≈0.4 g cm^{-3}).

For both carbon nanotubes and graphene, the introduction of surface functional groups such as oxygen[2,9,10,28,29] and

Dr. H. R. Byon
RIKEN Advanced Science Institute
2- 1 Hirosawa, Wako, Saitama 351-0198, Japan
B. M. Gallant, Dr. S. W. Lee, Prof. Y. Shao-Horn
Electrochemical Energy Lab
Department of Mechanical Engineering and Materials Science and Engineering
Massachusetts Institute of Technology
Cambridge, MA 02139, USA
E-mail: shaohorn@mit.edu

DOI: 10.1002/adfm.201200697

nitrogen[4,30,31] on carbon is a promising strategy to increase the energy density of electrodes while enabling high power performance and good cycle stability, opening up a new direction for design of electrodes. Previously, we showed that multiwalled carbon nanotubes (MWNTs) functionalized by amine can serve as pillars between graphene sheets in composite electrodes synthesized using the layer-by-layer (LbL) technique, which utilized electrostatic interactions between functional groups to develop self-assembled, thin film electrodes on a conducting indium tin oxide (ITO)-coated glass substrate that demonstrated high volumetric capacitance (160 F cm^{-3}) in aqueous electrolyte.[10] The LbL process enabled the development of conformal thin coatings with highly controllable thicknesses down to the nanometer scale, which is an important advantage for small-scale applications such as microsystems. However, the LbL process is time-consuming, and electrode thickness is limited to only several micrometers. To overcome the challenges of the LbL process, we recently reported[9] vacuum filtration of functionalized few-walled carbon nanotubes (VF-FWNTs) which enabled the development of free-standing and binder-free electrodes with thicknesses of ≈20 μm, utilizing a single component (functionalized FWNTs)[9] to demonstrate scalability of oxygen-functionalized FWNTs.

Here, we report a simple way to incorporate multiple electroactive nanocarbon components using vacuum filtration in order to make a hierarchical[25,26] functionalized MWNT/graphene structure with relatively high density (>1 g cm^{-3}) for the positive electrode of lithium batteries. As-prepared electrodes are shown by X-ray photoelectron spectroscopy (XPS) to contain diverse oxygen chemistries resulting from acid-functionalization of MWNTs (incorporating predominantly carbonyl, ester, and carboxylic groups) and from graphene oxide (GO) obtained by the oxiditative exfoliation of graphite (containing carbonyl, carboxylic, epoxide, and hydroxyl groups, among others).[32,33] The functionalized MWNTs and GO show a synergistic effect when combined in vacuum-filtrated electrodes, which might be associated with the electronic wiring of GO surfaces by functionalized MWNTs to enable reasonably high electronic conductivities for the electrodes (≈14 S cm^{-1}). We report that oxygen groups are active for Faradaic reactions at a potential of ≈3 V vs. Li, which can impart higher gravimetric currents and capacitances than pure double-layer charging. Importantly, the incorporation of two different nanocarbon materials, each with unique characteristic families of oxygen species, enables a novel capability for controlling the surface functionality of the carbon electrodes. Utilizing heat treatments in H_2/Ar (4/96%) gas, we report the selective removal of functional group species, which is shown to influence the electrochemical characteristics of the electrodes, opening new pathways for the design of electrodes with controlled surface chemistry.

2. Results and Discussion

2.1. Electrode Preparation

GO sheets were attained by oxidation and exfoliation of graphite powder using a modified Hummers method,[33–35] which produced single sheets with diverse oxygen functional groups and defect sites on GO.[33,36] It is believed that carbonyl, ester and carboxylic groups are situated at the edge (comprising 40% of the total oxygen functional groups, Supporting Information Figure S1) while considerable hydroxyl/epoxide groups are placed on the basal plane of the GO (60% of the total oxygen-functional groups, Supporting Information Figure S1).[37–39] GO sheets with high amounts of oxygen functional groups (≈45 at% of oxygen on carbon, Figure S1) are markedly stable and well dispersed in aqueous solution over a wide pH range.[10,33] MWNTs were purchased from NANOLAB (95% purity, outer diameter 15 ± 5 nm, length ≈1 to 5 μm). Negatively charged functionalized MWNTs (MWNT-COO^-) were prepared using surface functionalization processes described in previous work.[29] For electrode synthesis, aqueous dispersions were prepared containing either 1:10 or 1:1 weight ratio of functionalized MWNTs, which contain predominantly carbonyl, ester and carboxylic groups, and GO. The mixture of GO and functionalized MWNTs remained well dispersed at a pH of 5–6, and no agglomeration, precipitation, or phase separation could be observed over 3 days, implying a homogeneous mixture.

Hierarchical structures of as-prepared functionalized MWNT/GO were achieved through vacuum filtration of the mixed dispersion (**Figure 1**), which yielded flexible, free-standing and binder-free films with typical thicknesses of ≈5–10 μm, up to thicknesses of ≈70 μm. Scanning electron microscopy (SEM) images of resulting films showed a pillared structure (**Figure 2** and Supporting Information Figure S2) consisting of parallel and densely packed GO sheets with uniformly interspersed functionalized MWNTs, where the amount of MWNTs was clearly seen to increase upon increasing the MWNT:GO weight ratio from 1:10 (Figure 2b) to 1:1 (Figure 2c). In addition to the ease and simplicity of the single-step, room-temperature and aqueous-based process, the vacuum filtration method also allows for control over thickness, density, and composition of electrodes by varying the filtration volume and dispersion composition, respectively, enabling a facile synthesis of multicomponent nanocarbon-based structures with potentially tunable properties.

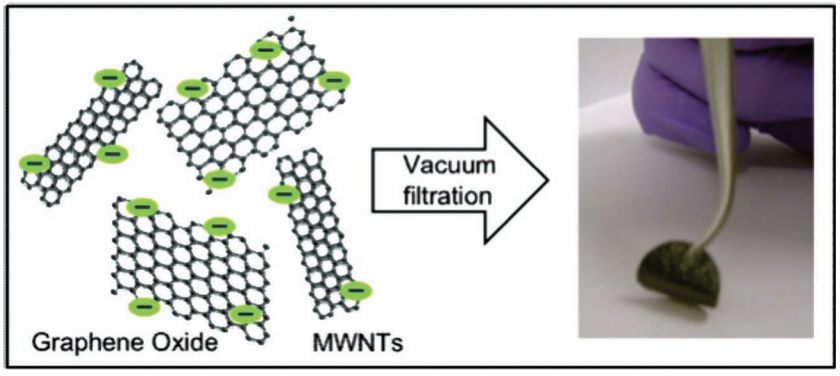

Figure 1. Schematic illustration of electrode synthesis from an aqueous dispersion of functionalized MWNTs and GO at room temperature (left). The resulting film of functionalized MWNT/GO is freestanding, binder-free, and flexible (right).

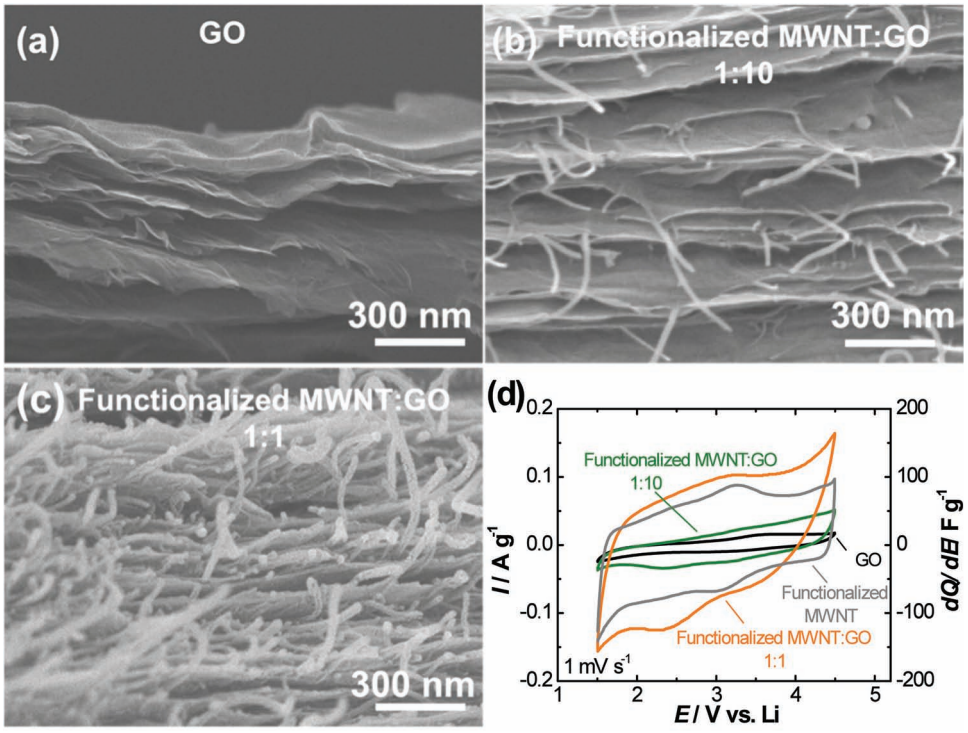

Figure 2. Cross-sectional SEM images of a) a GO film and b,c) MWNT/graphene films with functionalized MWNT:GO weight ratios of b) 1:10 and c) 1:1. d) Cyclic voltammetry (CV) comparison at 1 mV s^{-1} of the three films in (a–c) showing the influence of an increasing functionalized MWNT/GO weight ratio. A CV scan of functionalized MWNTs without GO, also prepared using the vacuum-filtration method, is shown for comparison in gray.

2.2 Surface Oxygen Control using Heat-Treatments and XPS Measurements

XPS was used to investigate the chemical identities of oxygen functional groups on as-prepared functionalized MWNT/GO electrodes (1:10 weight ratio). A survey scan (**Figure 3**) indicated a high oxygen content of 0.34 O/C while high-resolution scans revealed several oxygen species including hydroxyl/epoxide groups[10,40] (532.5 ± 0.2 eV in the O 1s spectrum, **Figure 4**d) and C–O[29,41] (286. 5 ± 0.1 eV in C 1s, Figure 4a), where all spectra were calibrated by setting the main peak in the C 1s binding energy (BE) region to the sp^2-hybridized carbons at 284.5 eV.

To attain selectivity over the chemistry of oxygen-containing functional groups on the electrodes, we heat treated as-prepared films at 200 °C or 900 °C in H_2/Ar (4/96%). The selective removal of oxygen species with heat treatment was confirmed by XPS (Figure 3,4). The atomic ratio of O/C decreased substantially to 0.18 after the heat treatment at 200 °C (Figure 3), where oxygen was removed mainly from GO as previous work showed that the oxygen content of functionalized MWNTs was not reduced greatly by heating treating in H_2 up to 300 °C.[2] Upon further heat treating to 900 °C in H_2/Ar, the O/C atomic ratio was reduced to 0.06, which presumably resulted from oxygen removal from both functionalized MWNTs and GO sheets. It should be mentioned that a very small amount of nitrogen was detected at 0.01–0.02 N/C, which was comparable among all electrodes and is believed to be derived from MWNT functionalization[29] utilizing HNO_3.

The remaining functional groups were identified from the C 1s and O 1s spectra and correlated to the heat treatment temperature. The C–O peak (286. 5 ± 0.1 eV) deconvoluted from the C 1s spectrum[29,41] in as-prepared films **(**Figure 4a) visibly decreased following the heat treatments at 200 °C (Figure 4b), which corresponds to decreasing hydroxyl/epoxide peak intensities (532.5 ± 0.2 eV) in the O 1s BE regions (Figure 4d–e). The resulting electrode had predominantly carbonyl (531.6 ± 0.1 eV) and ester (533.4 ± 0.1 eV)[40] among the oxygen species (Figure 4e), in addition to a relatively lower amount of carboxylic groups (534.4 ± 0.1 eV). The higher heat treatment temperature at 900 °C ensured the removal of a large fraction of oxygen functional groups (Figure 4c,f), leaving a largely reduced form of graphene (the total peak intensity in the O 1s BE regions in Figure 4f is magnified by 3x). Interestingly, the electrical conductivity of films was found to increase from 14.3 ± 1 S cm^{-1} for as-prepared films (1:1 weight ratio functionalized MWNT:GO, 10 μm) to 34.3 ± 5 S cm^{-1} for 200 °C heat-treated films with a comparable thickness (11.7 μm), which is consistent with removal of hydroxyl and epoxide groups on the basal plane of potentially insulating GO. The electrical conductivity of the 900 °C heat-treated film (65 μm) was even higher at 63.7 ± 0.5 S cm^{-1}, which could result from additional removal of defect sites related to oxygen functional groups such as carbonyl, ester and carboxylic groups as a result of heat treatment.

Cross-sectional SEM images of 200 °C and 900 °C heat-treated films showed that electrodes retained their original structure and did not undergo any dramatic change in hierarchical structure as a result of heat treatment (Supporting Information Figure S2).

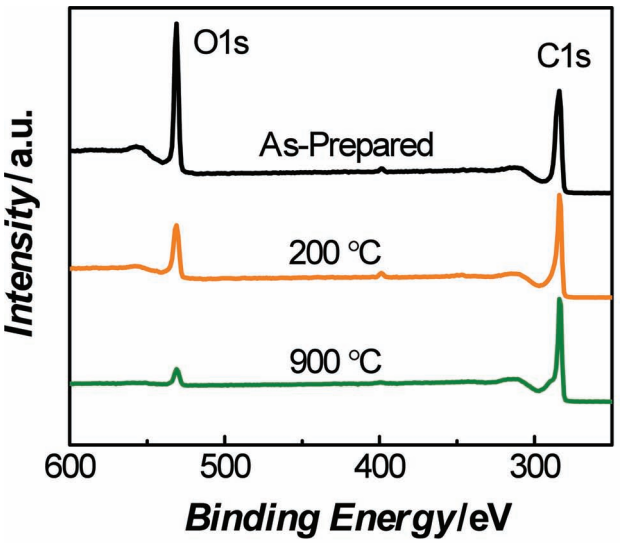

		Atomic %			Ratio	
Sample Name	Temp	C1s	O1s	N1s	O/C	N/C
As-Prepared	--	73.6	25.1	1.3	0.34	0.02
200 °C	200°C	83.1	15.2	1.7	0.18	0.02
900 °C	900°C	94.1	5.2	0.7	0.06	0.01

Figure 3. Top: XPS survey of as-prepared (black), 200 °C heat-treated electrodes (orange), and 900 °C heat-treated electrodes (green). Bottom: Corresponding atomic percentage concentrations of as-prepared and heat-treated electrodes.

The thickness, mass, and density of typical as-prepared and heat-treated electrodes (the diameter of all electrodes was 1.5 cm) examined electrochemically in **Figure 5**,**6** were 8.7 μm, 1.77 mg, 1.16 g cm^{-3} for as-prepared films, 4.0 μm, 1.37 mg, 1.94 g cm^{-3} for 200 °C heat-treated films, and 3.0 μm, 0.83 mg, 1.57 g cm^{-3} for 900 °C heat-treated films. Upon heat treatment at 200 °C, the electrode thickness decreased to less than half its original thickness owing to removal of hydroxyl/epoxide groups, enabling tighter packing of graphene sheets with increased density despite a mass decrease of 23%. After removal of carbonyl/carboxylic groups at 900 °C, the mass loss (75% decrease) is larger than that of thickness change (61% decrease), which could be related to carbonyl, ester, and carboxylic groups being lost from both the edge and basal plane sites, where all the removed groups contribute to the mass loss but only those associated with basal-plane sites greatly influence the thickness changes.

2.3. Electrochemical Characteristics of Freestanding Carbon Nanotube/Graphene Electrodes

Electrochemical cells were assembled using a lithium metal negative electrode, two Celgard 2500 separators with 1 M $LiPF_6$ (EC:DMC 3:7 v/v) electrolyte, and a vacuum-filtrated, functionalized carbon positive electrode. Owing to the freestanding and conductive nature of vacuum-filtrated films, no additional current collectors were attached during testing. First, we investigated the influence of functionalized MWNT addition on the electrochemical characteristics of vacuum-filtrated electrodes at low rates. Representative CV measurements at low rates such as 1 mV s^{-1} in Figure 2d show that vacuum-filtrated pure GO electrodes have very small current, while increasing functionalized MWNT addition in the electrode leads to substantial increases in the gravimetric current and capacitance. It is proposed that uniformly distributed functionalized MWNTs (diameter ≈15 nm) could pillar and separate GO sheets and increase the surface area of GO accessible to the electrolyte and thus the corresponding gravimetric capacitance. It is interesting to note that the gravimetric current and capacitance of as-prepared electrodes (1:1 weight ratio of functionalized MWNT:GO) were higher than that of vacuum-filtrated functionalized MWNT electrodes (Figure 2d), indicating that the GO and functionalized MWNTs might have a synergestic effect to enhance the electrochemically active surface area of vacuum-filtrated electrodes.

Electrodes heat-treated at 200 °C (Figure 5b) were found to yield higher gravimetric currents relative to the as-prepared electrode (Figure 5a), which could be attributed to increased electronic conductivities and thus electrochemically active surface area for charge storage. However, electrodes heat-treated at 900 °C (Figure 5c) had much reduced current, which could be attributed to the loss of surface oxygen functional groups (discussed in detail below), and the loss of surface area accessible to the electrolyte due to large changes in the microstructure as indicated by significant reduction in electrode thickness.

Voltage-dependent CV measurements in Figure 5a-c using electrodes prepared from the same initial batch of as-prepared electrodes show that the surface oxygen groups can be utilized to store charge Faradaically. For as-prepared and 200 °C heat-treated electrodes containing significant amounts of surface oxygen (Figure 3,4), the gravimetric current increased considerably (Figure 5a,b) when cycled in the wide voltage window 1.5–4.5 V vs. Li (black curve), compared to a restricted voltage window of 1.5–3.0 V vs. Li (green curve) or 3.0–4.5 V vs. Li (orange curve), similar to that found for functionalized FWNTs.[9] This finding indicates that below ≈3.0 V vs. Li, oxygen functional groups were electrochemically reduced by Li^+ ions and electrons and could be oxidized reversibly above ≈3.0 V vs. Li so that electrodes cycled over the full voltage range yielded higher gravimetric currents from the Faradaic reactions in addition to double-layer capacitance. In contrast, the gravimetric current of the 900 °C heat-treated electrode (Figure 5c) was nearly the same regardless of the scan window. These observations are in agreement with XPS results, which indicate that the majority of oxygen-containing groups are removed following the heat treatment at 900 °C. Since oxygen groups contribute substantially to the gravimetric current via Faradaic reactions, the 900 °C heat-treated electrodes without functional groups yield lower gravimetric currents and potential-independent behavior, indicative of double-layer capacitance only. It is noted that a significant increase in gravimetric current was found between the first (dashed green; first cycle from OCV after cell assembly) and final (solid green; conducted after all other scans shown) curves for both as-prepared and 200 °C heat-treated electrodes, which is believed to be related to increased electrolyte

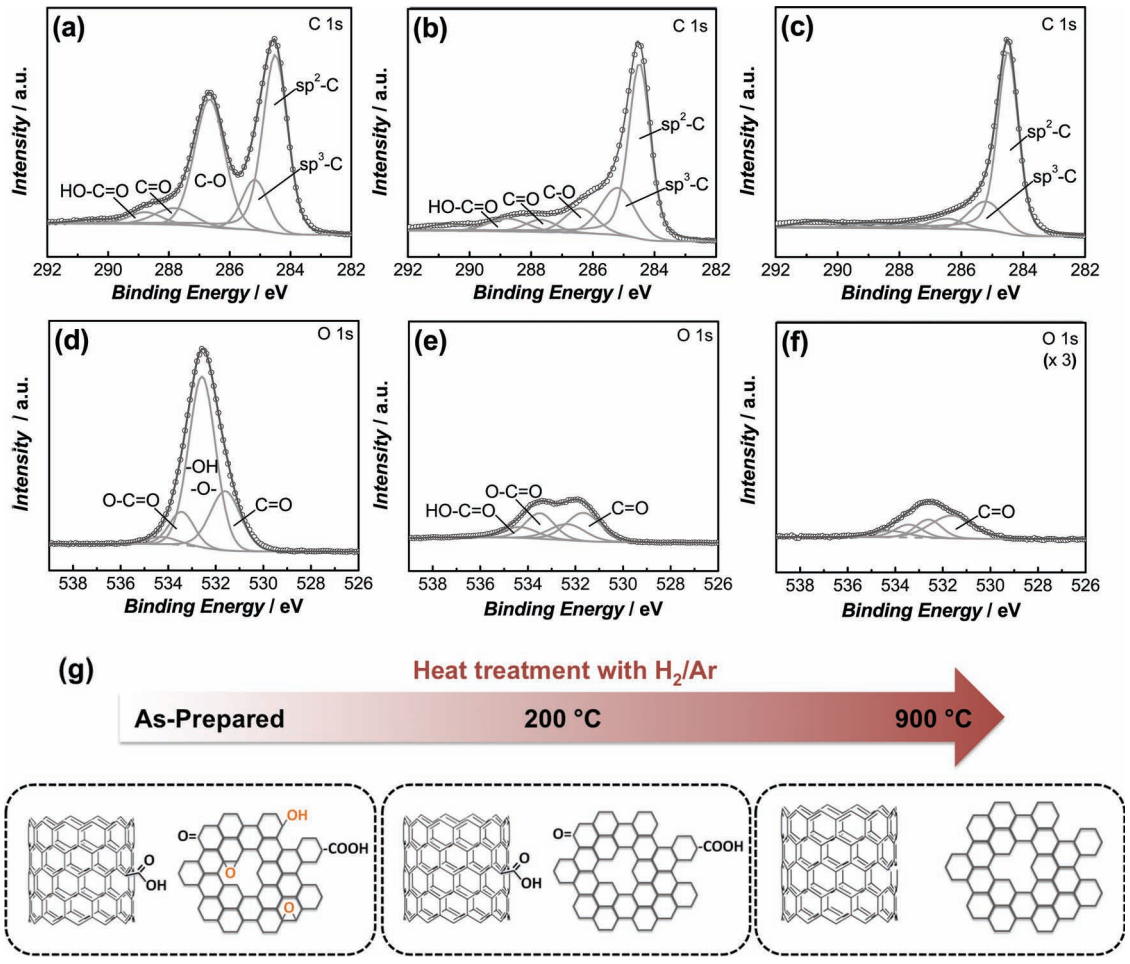

Figure 4. XPS: a–c) C 1s and d–f) O 1s binding energy (BE) regions of a,d) as-prepared, b,e) 200 °C, and c,f) 900 °C heat-treated films. The intensity of O 1s of the 900 °C heat-treated film (f) is magnified by 3 times. All spectra were calibrated by setting the main peak in the C 1s BE region to the sp^2-hybridized carbons at 284.5 eV. Predominant oxygen functional groups were identified in the O 1s BE regions as hydroxyl/epoxide (532.5 ± 0.2 eV) on as-prepared films, and carbonyl (531.6 ± 0.1 eV), carboxylic (534.4 ± 0.1 eV), and ester (533.4 ± 0.1 eV)[40] groups on 200 °C heat-treated films. g) Schematics of oxygen functional groups on functionalized MWNTs and GO in as-prepared films (left) and heat-treated at 200 °C (center) and 900 °C (right) in H_2/Ar.

wetting of the electrode surface, which could increase the accessible surface area and thus yield a higher current. This cycle-dependent effect was not observed in recently-reported vacuum filtrated, functionalized FWNT electrodes under the same testing conditions,[9] further suggesting that this effect is related to the microstructure of these freestanding carbon nanotube/graphene electrodes.

We quantified the double-layer capacitance and total (double-layer + Faradaic) capacitance using the gravimetric current at 4 V vs. Li in the positive scan direction for the orange and black curves in Figure 5a–c, respectively. For as-assembled electrodes, the double-layer and Faradaic capacitances were 60 and 51 F g^{-1} (70 and 58 F cm^{-3}), as shown in Figure 5d. Upon heat-treatment at 200 °C, the double-layer capacitance increased to 98 F g^{-1} (190 F cm^{-3}) while the Faradaic contribution remained nearly constant at 60 F g^{-1} (118 F cm^{-3}). It is interesting to note that the increase in total gravimetric capacitance of 200 °C heat-treated electrodes relative to as-prepared electrodes can be nearly attributed to the increase in double-layer capacitance while the higher Faradaic and double-layer volumetric capacitances for 200 °C heat-treated electrodes is owing to a higher density (1.9 g cm^{-3}) than that (1.2 g cm^{-3}) of as-assembled electrodes. The maximum total gravimetric capacitance in this study of 155 F g^{-1}, obtained from MWNT/graphene electrodes heat-treated at 200 °C, is roughly comparable to those of activated graphene[27] (≈160 F g^{-1}) and single wall carbon nanotubes (SWNTs)[24] (≈160 F g^{-1}), and is lower than that of conducting-paper electrodes[8] (200 F g^{-1}, considering the weight of CNTs only) in organic electrolytes reported recently. However, owing to an unusually high mass density, the total volumetric capacitance of 307 F cm^{-3} for 200 °C heat-treated electrodes is 3–5 times higher than reported works including carbide-derived carbons with comparable thickness.[22] Finally, the Faradaic contribution from 900 °C heat-treated electrodes was nearly absent and the double-layer and Faradaic gravimetric capacitances of 46 and 15 F g^{-1} (72 and 24 F cm^{-3}) were much lower than those of as-prepared and 200 °C heat-treated electrodes.

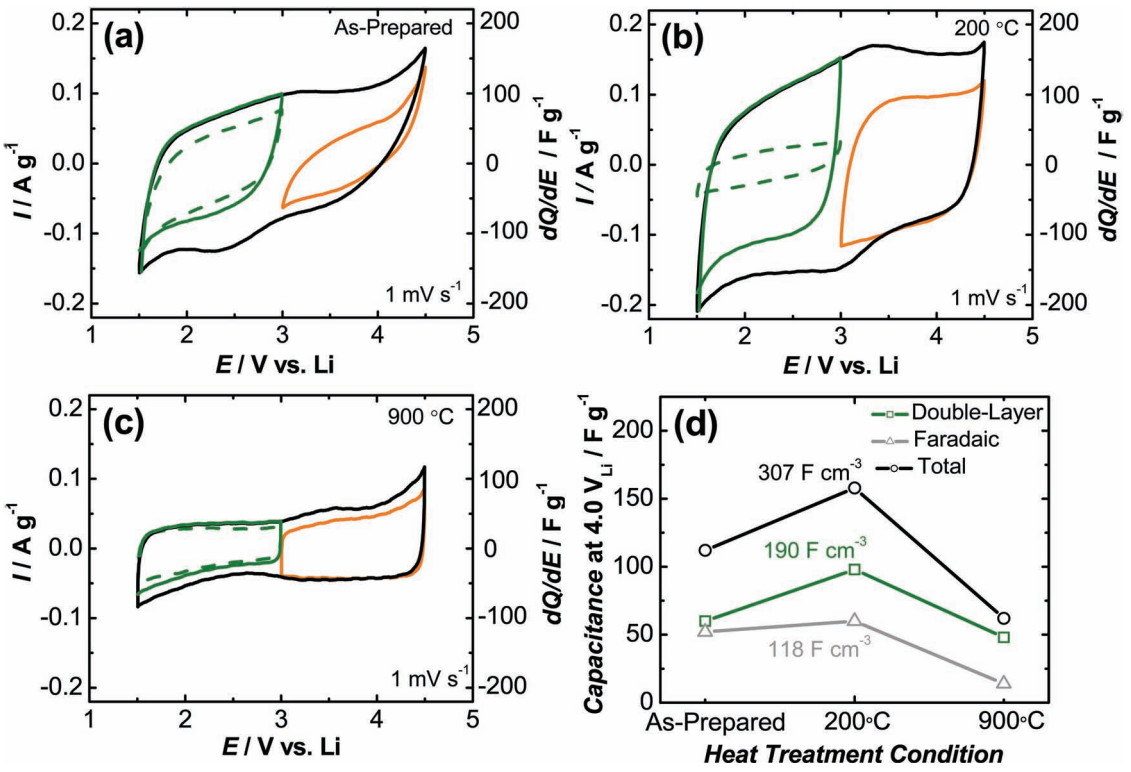

Figure 5. Potential-dependent cyclic voltammetry (1 mV s^{-1}) of a) as-prepared electrodes (8.7 µm), b) 200 °C heat-treated electrodes (4 µm), and c) 900 °C heat-treated electrodes (3 µm). All films were made from the same batch (1:1 weight ratio of functionalized MWNT:GO) with different heat-treatment temperatures. The green dotted line is the first scan after cell assembly and the solid green curve is the final scan after all other cycles were conducted. d) Relative contribution of double-layer and Faradaic capacitance to total capacitance as a function of heat-treatment condition. The double-layer capacitance was obtained from (a–c) as the gravimetric current at 4 V vs. Li on the positive scan (orange curve corresponding to cycling between 3.0–4.5 V vs. Li in the double-layer regime) divided by the scan rate, while the total capacitance was obtained in a similar manner from (a–c) for the black curve (cycling between 1.5–4.5 V vs. Li). The Faradaic capacitance is the difference between the total and double-layer contributions. The volumetric capacitance contributions for the 200 °C heat-treated sample (density = 1.94 g cm^{-3}) are noted in the figure.

CV measurements also provide insights into equilibrium voltages of Faradaic reactions associated with lithiation of different surface functional groups on carbon (Figure 5 and Supporting Information Figure S3). CV data of 200 °C heat-treated electrodes at 1 mV s^{-1} show nearly reversible reduction (≈3.0 V vs. Li) and oxidation (≈3.4 V vs. Li) peaks (black solid line in Figure 5b). This Faradaic reaction with an equilibrium voltage of ≈3.2 V vs. Li can be attributed to reactions between Li^+ and carbonyl, ester and carboxylic groups such as $Li^+ + C{=}O_{MWNT/graphene\ 200\ °C} + e^- \leftrightarrow C\text{-}O\text{-}Li_{MWNT/graphene\ 200\ °C}$.[2,29] In contrast, the reduction peak of as-prepared electrodes was shifted to ≈2.5 V vs. Li while the oxidation peak was not very visible, having the highest currents at ≈3.1 V vs. Li, which may suggest an equilibrium potential of 2.8 V for the lithiation of epoxide and hydroxyl groups found predominantly (Figure 4). The large voltage difference between reduction and oxidation, which was observed even at a lower scan rate of 0.1 mV s^{-1} (Supporting Information Figure S3), suggests that the kinetics of lithiation/delithiation of epoxide and hydroxyl groups is sluggish in as-prepared electrodes. Further studies are needed to verify the proposed voltages of lithiation for these surface functional groups.

Galvanostatic rate-capability testing of the vacuum-filtrated electrodes (Figure 6) showed a similar trend to that observed from CV measurements at low rates, with slightly higher gravimetric capacity obtained for electrodes heat-treated at 200 °C (≈135 mAh g^{-1}) compared to as-prepared electrodes (≈110 mAh g^{-1}), and substantially lower capacity obtained for electrodes heat-treated at 900 °C (≈30 mAh g^{-1}) and functionalized MWNTs (Supporting Information Figure S4). This difference cannot be explained well by the difference in the C/O ratio for these electrodes (Figure 6d), which suggests that the surface area accessible to electrochemical reactions played an important role. It is interesting to note that the volumetric capacity of 200 °C heat-treated electrodes is very large (260 mAh cm^{-3}), which is greater than that of LbL-MWNT/Graphene (1.3 µm),[28] LbL-MWNT/Polyaniline (PANi) (1.3 µm),[42] and vacuum-filtrated functionalized FWNTs (15–22 µm)[9] reported recently owing to a substantially higher mass density. The gravimetric capacities of as-prepared and 200 °C heat-treated electrodes could be well retained over 100 cycles, as shown in Supporting Information Figure S5. The initial capacity reduction of as-prepared electrodes might result from irreversible oxidation of epoxide and hydroxyl groups above ≈4 V vs. Li (oxidation currents shown in Figure 5a).

The gravimetric capacities decreased with increasing rates, where significant reduction was noted at 10 A g^{-1}. While as-prepared and 200 °C heat-treated electrodes showed higher gravimetric capacities at low gravimetric currents (<1 A g^{-1}),

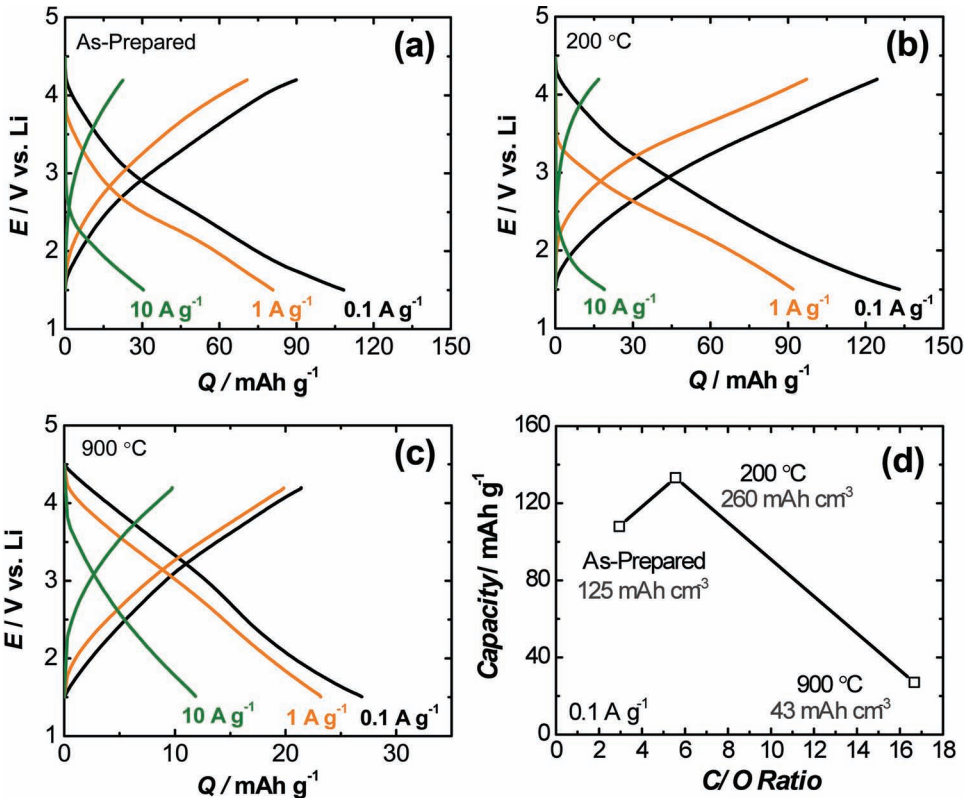

Figure 6. Galvanostatic discharge/charge curves of a) as-prepared (8.7 µm), b) 200 °C heat-treated electrodes (4 µm), and c) 900 °C heat-treated electrodes (3 µm) having a 1:1 weight ratio of functionalized MWNT:GO at 0.1, 1, and 10 A g^{-1}. Prior to each galvanostatic charge or discharge, the electrodes were held at 1.5 or 4.5 V, respectively, for 1 h. All films were made from the same batch with different heat-treatment temperatures. d) Discharge capacity at 0.1 A g^{-1} as a function of C/O ratio (a–c). The corresponding volumetric capacities are labeled in the figure.

their capacities were comparable to that of 900 °C heat-treated electrodes and functionalized MWNTs at higher currents (10 A g^{-1}), as shown in **Figure 7**a. This suggests that oxygen functional groups, which were accessed at low rates, could not be accessed at high currents. This rate performance in Figure 7a was sustained for electrode thicknesses up to ≈20 µm (Supporting Information Figure S6 and S7). It should be mentioned that our current lithium cell configuration is optimized for electrodes with thickness below ≈20 µm. It is noted that a substantial decrease in the attainable gravimetric capacity was obtained for electrodes with thicknesses above ≈60 µm, possibly due to the increase of electronic and ionic resistances or the insufficient infiltration of electrolyte into the electrodes. Future research will focus on optimizing the lithium cell setup for better performance at higher thicknesses. The gravimetric energy and power performance of these electrodes (based on the positive electrode weight only) was determined subsequently from galvanostatic data (Figure 6) and is shown in a Ragone Plot in Figure 7b. At relatively low power (≈2.6 kW kg^{-1}), the gravimetric energy of as-prepared (≈190 Wh kg^{-1}) and 200 °C heat-treated (≈230 Wh kg^{-1}) electrodes were comparable to vacuum-filtrated functionalized FWNTs[9] and other electrodes reported

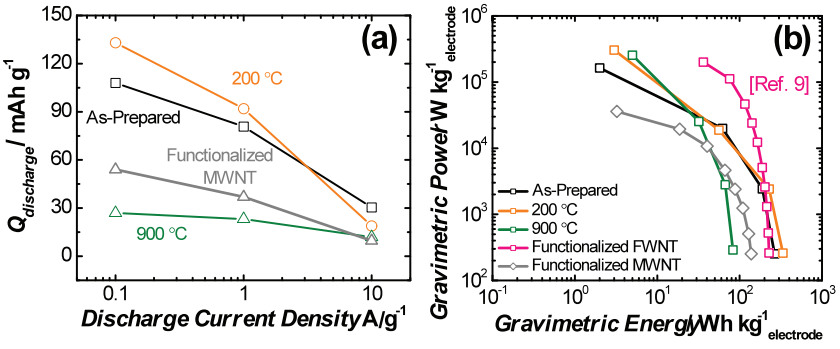

Figure 7. a) Gravimetric discharge capacity of the samples in Figure 6 as a function of gravimetric current for as-prepared, 200 °C, and 900 °C heat-treated electrodes, and comparison with functionalized MWNT electrodes similarly assembled using the vacuum filtration method. b) Ragone plot of gravimetric energy and power performance of MWNT/graphene electrodes (green, orange, and black squares) obtained from gravimetric discharge data in Figure 6a–c. For comparison, the energy-power performance of vacuum-filtrated functionalized FWNT (22 µm)[9] and functionalized MWNT (75 µm) electrodes is shown.

previously.[28,43] When considering scale-up to full devices, where the packaged mass is projected to be 5-8 times that of the positive electrode,[2,28] the gravimetric energy of MWNT/graphene electrodes could have comparable or slightly lower gravimetric energy compared to current Li-ion cells (Supporting Information Figure S8) and power capabilities that exceed that of current Li-ion (10 Wh/kg_{device} at ≈3 kW/kg_{device}). More interestingly, the volumetric energy of as-prepared and 200 °C heat-treated electrodes is substantially higher than functionalized FWNT electrodes (Supporting Information Figure S9). For example, ≈450 Wh L^{-1} was found for 200 °C heat-treated electrodes at ≈5 kW L^{-1}. Therefore, the combination of high gravimetric energy density and a high mass density of 1.94 g cm^{-3} achieved for 200 °C heat-treated films imparts a considerable volumetric performance advantage for these electrodes relative to previous work.[8,11,24] However, as-prepared and 200 °C heat-treated electrodes have lower rate capability than functionalized FWNTs. The relatively rapid loss of energy with increasing power found for vacuum-filtrated as-prepared and 200 °C heat-treated functionalized MWNT/graphene electrodes might be attributed to higher electrode densities (>1 g cm^{-3}) than those of functionalized FWNTs (≈0.4 g cm^{-3}), where Li^+ ion mobility in the electrolyte may become rate-limiting at high power.

3. Conclusions

We synthesized self-standing, binder-free functionalized MWNT/graphene electrodes with a hierarchical structure via vacuum filtration for use as positive electrodes in lithium batteries. Faradaic contributions from electrochemically active carbonyl, carboxylic and ester groups and electrical double-layer capacitance can provide gravimetric energies of ≈230 Wh kg^{-1} at ≈2.6 kW kg^{-1} (≈450 Wh L^{-1} at ≈5 kW L^{-1}) by tuning of the surface oxygen chemistry via heat treatment at 200 °C in H_2/Ar. Addition of graphene in the electrodes can allow the synthesis of self-standing films with thickness as thin as a few micrometers and increase the electrode density (>1 g cm^{-3}) relative to electrodes with MWNTs only (≈0.8 g cm^{-3}). The high densities of MWNT/graphene electrodes yield exceptionally high volumetric energy densities at low rates relative to electrodes of functionalized MWNTs and FWNTs[9] but at the expense of rate capability. Developing hierarchical electrodes based on functionalized graphene and MWNTs with tunable surface chemistry and microstructure presents an interesting pathway to design electrodes for lithium battery and electrochemical capacitor applications.

4. Experimental Section

GO Synthesis: GO solution was made using a modified Hummers method.[33,34,35] Briefly, 1 g of raw graphite powder (SP-1, Bay Carbon), 0.5 g of $K_2S_2O_8$ (Fluka), and 0.5 g of P_2O_5 (Fluka) were stirred in 3 mL of H_2SO_4 at 80 °C for 4.5 h and copiously washed and dried in air overnight. Then 3 g of $KMnO_4$ (Sigma-Aldrich) was slowly added to the graphite powder solution with 23 mL of H_2SO_4 at 0 °C. After vigorous stirring at 36 °C for 2 h, 46 mL of deionized water (DI water, R ≈ 18.2 MΩ) was added at 0 °C and the solution was stirred at 36 °C for additional 2 h. The oxidation step was completed by the addition of 140 mL of DI water and 2.5 mL of H_2O_2 solution (35%). The GO solution (brown color) was washed, and filtrated with 250 mL of HCl (10%). Before complete drying, the GO was dispersed in DI water (10 mg mL^{-1}) and dialyzed for 2 weeks, from which pH values attained ≈4 to 6.

Functionalized MWNT Synthesis: Functionalization of MWNT was performed using a previously reported method.[29] Briefly, functionalized MWNTs were prepared by oxidizing pristine MWNTs (95% purity, 400 m^2 g^{-1}, NANOLAB) in a mixture of H_2SO_4 (96.5%, J. T. Baker) and HNO_3 (70%, Mallinckrodt Chemicals) solution (3:1 v/v) at 70 °C for 2 h. The functionalized MWNTs were washed in 5% of HCl solution and dried in air. The dried powder was dispersed in DI water by stirring and sonication (1 mg mL^{-1}).

Assembly of Functionalized MWNT/GO Electrodes and Heat-Treatment: For electrodes with a 1:1 weight ratio of functionalized MWNT:GO, the dialyzed GO solution (10 mg mL^{-1}) and functionalized MWNTs (1 mg mL^{-1}) solutions were mixed with 1:9 (v/v) ratio and sonicated at 100 W for 1 h and stirred for 1 h. Electrodes with a 1:10 weight ratio were prepared similarly with appropriately adjusted volumes of functionalized MWNTs and GO. The mixture was well dispersed in DI water over 3 days without any precipitation or aggregation. The mixture was vacuum-filtrated using a filtration membrane with 0.5 µm pore size and 47 or 90 mm diameter (PC, Whatman). To make ≈6, 70, and 250 µm as-prepared films, approximately 30, 110, and 250 mL of functionalized MWNT/GO solution was used, respectively, indicating that the thickness and density of films can be controlled by varying the filtration volume. Following filtration, the air-dried film was peeled off from the filtration membrane and dried in a convection oven at 60 °C for 24 h.

Heat Treatment Conditions: For the preparation of 200 °C and 900 °C heat-treated electrodes, in which the GO was converted to reduced graphene oxide, the as-prepared film was heat-treated at the indicated temperature for 2 h at 10 °C min^{-1} ramp rate and under 20 cc min^{-1} of H_2/Ar (4/96%) gas flow, then cooled down to room temperature.

Characterization: The cross-sectional views of all films were investigated using SEM (JEOL 6700) after sputtering the films with Au/Pd (≈1 nm). Chemical identification of films was addressed by XPS using a Kratos AXIS ultra imaging monochromatic Al anode. All spectra were calibrated by setting the C 1s photoemission peak for sp^2-hybridized carbons to 284.5 eV, and were fitted after a Shirley type background subtraction. Sheet-resistance was measured by a 4-point probe (Signatone S-302-4) with a device analyzer (Keithley 4200).

Electrochemical Testing: Electrochemical cells (Tomcell, Japan) were prepared with a lithium metal negative electrode, two microporous separators (Celgard 2500, 25 µm thickness) wetted with 1 M $LiPF_6$ in EC:DMC (3:7 v/v) electrolyte (140 µL total), and a MWNT/graphene positive electrode (15 mm diameter). The film thickness was measured by a Digimatic Micrometer (Mettler Toledo) in three different locations on the film and mass was obtained by a balance (Mettler Toledo). Cyclic voltammetry, galvanostatic, and cycling tests were conducted in the voltage range 1.5–4.5 V vs. Li. For cells tested under galvanostatic conditions, the voltage was held constant at 1.5 V or 4.5 V for 1 h prior to charge or discharge, respectively. In all cases, values normalized on a per-gram basis consider the weight of active material in the positive electrode only.

Supporting Information

Supporting Information is available from the Wiley Online Library or from the author.

Acknowledgements

H.R.B. and B.M.G. contributed equally to this work. The authors thank Ethan J. Crumlin for collecting XPS data. The authors acknowledge support from Contour Energy Systems for this project, and the MRSEC

Program of the National Science Foundation under award number DMR - 0819762. B.M.G. acknowledges a graduate research fellowship from the National Science Foundation.

Received: March 13, 2012
Revised: April 24, 2012
Published online: June 8, 2012

[1] J. R. Miller, A. F. Burke, *ECS Interface* **2008**, *17*, 53.
[2] S. W. Lee, N. Yabuuchi, B. M. Gallant, S. Chen, B.-S. Kim, P. T. Hammond, Y. Shao-Horn, *Nat. Nanotechnol.* **2010**, *5*, 531.
[3] J. M. Tarascon, M. Armand, *Nature* **2001**, *414*, 359.
[4] G. Lota, K. Fic, E. Frackowiak, *Energy Environ. Sci.* **2011**, *4*, 1592.
[5] P. Simon, A. F. Burke, *ECS Interface* **2008**, *17*, 38.
[6] P. Simon, Y. Gogotsi, *Nat. Mater.* **2008**, *7*, 845.
[7] D. N. Futaba, K. Hata, T. Yamada, T. Hiraoka, Y. Hayamizu, Y. Kakudate, O. Tanaike, H. Hatori, M. Yumura, S. Iijima, *Nat. Mater.* **2006**, *5*, 987.
[8] L. Hu, J. W. Choi, Y. Yang, S. Jeong, F. L. Mantia, L.-F. Cui, Y. Cui, *Proc. Natl. Acad. Sci. USA* **2009**, *106*, 21490.
[9] S. W. Lee, B. M. Gallant, Y. Lee, N. Yoshida, D. Y. Kim, Y. Yamada, S. Noda, A. Yamada, Y. Shao-Horn, *Energy Environ. Sci.* **2012**, *5*, 5437.
[10] H. R. Byon, S. W. Lee, S. Chen, P. T. Hammond, Y. Shao-Horn, *Carbon* **2011**, *49*, 457.
[11] M. D. Stoller, S. Park, Y. Zhu, J. An, R. S. Ruoff, *Nano Lett.* **2008**, *8*, 3498.
[12] D. Wang, R. Kou, D. Choi, Z. Yang, Z. Nie, J. Li, L. V. Saraf, D. Hu, J. Zhang, G. L. Graff, J. Liu, M. A. Pope, I. A. Aksay, *ACS Nano* **2010**, *4*, 1587.
[13] D.-W. Wang, F. Li, J. Zhao, W. Ren, Z.-G. Chen, J. Tan, Z.-S. Wu, I. Gentle, G. Q. Lu, H.-M. Chen, *ACS Nano* **2009**, *3*, 1745.
[14] Y. Wang, Z. Shi, Y. Huang, Y. Ma, C. Wang, M. Chen, Y. Chen, *J. Phys. Chem. C* **2009**, *113*, 13103.
[15] Q. Wu, Y. Xu, Z. Yao, A. Liu, G. Shi, *ACS Nano* **2010**, *4*, 1963.
[16] D. Yu, L. Dai, *J. Phys. Chem. Lett.* **2010**, *1*, 467.
[17] A. Alonso, V. Ruiz, C. Blanco, R. Santamara, M. Granda, R. Menendez, S. G. E. de Jager, *Carbon* **2006**, *44*, 441.
[18] D. Pech, M. Brunet, P.-L. Taberna, P. Simon, N. Fabre, F. Mesnilgrente, V. Conédéra, H. Durou, *J. Power Sources* **2010**, *195*, 1266.
[19] L. L. Zhang, X. S. Zhao, *Chem. Soc. Rev.* **2009**, *38*, 2520.
[20] D. Pech, M. Brunet, H. Durou, P. H. Huang, V. Mochalin, Y. Gogotsi, P.-L. Taberna, P. Simon, *Nat. Nanotechnol.* **2010**, *5*, 651.
[21] J. Chmiola, C. Largeot, P.-L. Taberna, P. Simon, Y. Gogotsi, *Angew. Chem. Int. Ed.* **2008**, *47*, 3392.
[22] J. Chmiola, C. Largeot, P.-L. Taberna, P. Simon, Y. Gogotsi, *Science* **2010**, *328*, 480.
[23] J. Chmiola, G. Yushin, Y. Gogotsi, C. Portet, P. Simon, P. L. Taberna, *Science* **2006**, *313*, 1760.
[24] A. Izadi-Najafabadi, S. Yasuda, K. Kobashi, T. Yamada, D. N. Futaba, H. Hatori, M. Yumura, S. Iijima, K. Hata, *Adv. Mater.* **2010**, *22*, E235.
[25] C. X. Guo, C.M Li, *Energy Environ. Sci.* **2011**, *4*, 4504.
[26] C. X. Guo, H. B. Yang, Z. M. Sheng, Z. S. Lu, Q. L. Song, C. M. Li, *Angew. Chem. Int. Ed.* **2010**, *49*, 3014.
[27] Y. W. Zhu, S. Murali, M. D. Stoller, K. J. Ganesh, W. W. Cai, P. J. Ferreira, A. Pirkle, R. M. Wallace, K. A. Cychosz, M. Thommes, D. Su, E. A. Stach, R. S. Ruoff, *Science* **2011**, *332*, 1537.
[28] S. W. Lee, B. M. Gallant, H. R. Byon, P. T. Hammond, Y. Shao-Horn, *Energy Environ. Sci.* **2011**, *4*, 1972.
[29] S. W. Lee, B.-S.Kim, S. Chen, Y. Shao-Horn, P. T. Hammond, *J. Am. Chem. Soc.* **2009**, *131*, 671.
[30] E. Frackowiak, *Phys. Chem. Chem. Phys.* **2007**, *9*, 1774.
[31] G. Lota, B. Grzyb, H. Machnikowska, J. Machnikowski, E. Frackowiak, *Chem. Phys. Lett.* **2005**, *404*, 53.
[32] A. Lerf, H. Y. He, M. Forster, J. Klinowski, *J. Phys. Chem. B* **1998**, *102*, 4477.
[33] D. Li, M. B. Müller, S. Gilje, R. B. Kaner, G. G. Wallace, *Nat. Nanotechnol.* **2008**, *3*, 101.
[34] W. S. Hummers, R. E. Offeman, *J. Am. Chem. Soc.* **1958**, *80*, 1339.
[35] N. I. Kovtyukhova, P. J. Ollivier, B. R. Martin, T. E. Mallouk, S. A. Chizhik, E. V. Buzaneva, A. D. Gorchinskiy, *Chem. Mater.* **1999**, *11*, 771.
[36] D. A. Dikin, S. Stankovich, E. J. Zimney, R. D. Piner, G. H. B. Dommett, G. Evmenenko, S. T. Nguyen, R. S. Ruoff, *Nature* **2007**, *448*, 457.
[37] O. C. Compton, D. A. Dikin, K. W. Putz, C. Brinson, S. T. Nguyen, *Adv. Mater.* **2010**, *22*, 892–896.
[38] S. Stankovich, D. A. Dikin, R. D. Piner, K. A. Kohlhaas, A. Kleinhammes, Y. Jia, Y. Wu, S. T. Nguyen, R. S. Ruoff, *Carbon* **2007**, *45*, 1558.
[39] S. Stankovich, R. D. Piner, X. Chen, N. Wu, S. T. Nguyen, R. S. Ruoff, *J. Mater. Chem.* **2006**, *16*, 155.
[40] U. Zielke, K. J. Hüttinger, W. P. Hoffman, *Carbon* **1996**, *34*, 983.
[41] S. Kundu, Y. Wang, W. Xia, M. Muhler, *J. Phys. Chem. C* **2008**, *112*, 16869.
[42] M. N. Hyder, S. W. Lee, F. B. Cebeci, D. J. Schmidt, Y. Shao-Horn, P. T. Hammond, *ACS Nano* **2011**, *5*, 8552.
[43] N. Dudney, *ECS Interface* **2008**, *17*, 44.